# *Articles*

# Molecular Orbital Study of the Mechanism of Platinum(0)-Catalyzed Alkene and Alkyne Diboration Reactions

Qiang Cui, Djamaladdin G. Musaev, and Keiji Morokuma*

*Cherry L. Emerson Center for Scientific Computation and Department of Chemistry, Emory University, Atlanta, Georgia 30322*

*Received October 10, 1996*[⊗]

A theoretical study has been carried out for the mechanism of Pt(0)-catalyzed alkyne and alkene diboration reactions with the B3LYP density functional method. Two different paths are studied, path A where the first step is B−B oxidative addition and path B where the first step is alkyne/alkene coordination. Though the coordination energy of acetylene and ethylene to $Pt(PH_3)_2$ is larger than the energy gain of oxidative addition of $(OH)_2B-B(OH)_2$ to $Pt(PH_3)_2$, the trend reverses as the size of substituents on alkynes, alkenes, and $(OH)_2B-B(OH)_2$ increases, and for large alkynes path A is expected to be favored over path B. Path A has been shown to proceed via the following steps: (a) coordination of $(OH)_2B-B(OH)_2$ to $Pt(PH_3)_2$, (b) oxidative addition of the B−B bond to Pt, (c) dissociation of one phosphine ligand, (d) coordination of alkyne/alkene to form a $\pi$-complex, (e) migratory insertion of alkyne/alkene into a Pt−B bond, (f) migration of the $CH_xCH_xB(OH)_2$ ($x = 1$ or 2) group to become *cis* to $B(OH)_2$, (g) recoordination of phosphine, and (h) elimination of $(OH)_2BCH_x-CH_xB(OH)_2$ product. The rate-determining step is found to be phosphine dissociation step c, in agreement with the experiment. The observed difference between alkyne and alkene diboration reactions originates from the difference in energetics in the step e and has been explained in terms of lower deformation energy and larger B−C $\sigma$ bond energy for alkyne than for alkene in $(B(OH)_2)(PH_3)Pt-CH_xCH_x-B(OH)_2$. The experimental stereoselectivity has been explained in terms of rigidity of the C−C $\pi$ bond.

## I. Introduction

Transition-metal-catalyzed alkene and alkyne boration reactions are attractive methods to produce alkyl- or alkenylboron derivatives with defined regio- and stereochemistry and provide opportunities for applications of boron derivatives in synthetic organic chemistry.[1] Although the catalytic hydroboration of alkenes and alkynes with catecholborane or polyhedral boranes has been extensively studied by experimental[1] and theoretical[2] methods, the catalytic alkene and alkyne diboration reactions have just begun to be explored.[3] It should be noted that uncatalyzed addition of diborane $H_2B-BH_2$ to alkenes and alkynes are well-documented[4] to have two drawbacks which hamper their utility as synthetic reagents: the difficulties in preparation and the inherent instability of these compounds.

In contrast to the halide species, derivatives which contain oxygen and nitrogen functionality are stable but much less reactive.[5] However, the recently reported Pt(0)-catalyzed alkyne diboration reaction with pinacol ester derivatives showed high regio- and stereoselectivity and occurred with high yield.[3] In general, it has been demonstrated that (i) *cis* addition of the B−B bond in pinacol ester derivatives, $(OCH_2)_2B-B(CH_2O)_2$, to alkynes can be catalyzed by a Pt(0) complex, (ii) $(PPh_3)_2$-Pt(bisboryl) and $(PPh_3)_2Pt$(ethylene) are more efficient catalyst precursors than $Pt(PPh_3)_4$ for the diboration of alkynes, (iii) $B_2cat_2$ (cat = catecol) reacts faster than $B_2pin_2$ (pin = pinacol), which in turn reacts much faster than $B_2(4\text{-}t\text{-Bu-cat})_2$, and (iv) internal alkynes react much faster than terminal alkynes regardless of the diboron reagent used. It is believed that the phosphine dissociation is the rate-determining step of the entire reaction. However, there remain several questions including the following: (i) What is the role of phosphine in the later stages of the catalytic cycle? (ii) What are the structure and energetics of the assumed intermediates and transition states involved in the reaction? (iii) Why do Pt(0) complexes catalyze alkyne diboration but not alkene diboration? We believe that high level quantum chemical calculations, together with experiment, are very useful in solving these and other related problems.

Therefore, in the present paper we have studied using a density functional method the $Pt(PH_3)_2$-catalyzed acetylene and ethylene diboration reaction by $(HO)_2B-B(OH)_2$ by calculating the potential energy surfaces (PESs) of the reactions

$$Pt(PH_3)_2 + C_2H_2 + R_2B-BR_2 \rightarrow Pt(PH_3)_2 + (R_2B)CH{=}CH(BR_2) \quad (1)$$

and

[⊗] Abstract published in *Advance ACS Abstracts,* March 1, 1997.

S0276-7333(96)00860-6 CCC: $14.00 

$$Pt(PH_3)_2 + C_2H_4 + R_2B{-}BR_2 \rightarrow Pt(PH_3)_2 + (R_2B)CH_2{-}CH_2(BR_2) \quad (2)$$

where R = OH. Here, $(HO)_2B{-}B(OH)_2$ and $PH_3$ are models for $(OCH_2)_2B{-}B(CH_2O)_2$ and $PPh_3$, respectively, used in the experiment. It has been shown in our previous paper[2a] that $HB(OH)_2$ is a reasonable model for HBcat, and therefore, we believe that $(HO)_2B{-}B(OH)_2$ is also a good model for pinacol ester.

In section II, the methods of computation are described along with discussions of the structure and stabilities of the reactants. In section III, we discuss the structure and energetics of the intermediates and transition states involved. In section IV, we compare the PESs of the reactions 1 and 2. In the final section we present a few conclusions.

## II. Calculation Procedure and the Evaluation of the Approximations

Geometries of the stationary points on the PES of the reactions 1 and 2 are optimized using the B3LYP hybrid density functional theory[6] with a standard double-ζ quality basis sets (denoted below as BSI), which consists of lanl2dz associated with the relativistic effective core potential (ECP) for Pt and the nonrelativistic ECP for P and D95 for the other atoms.[7] The energies shown in the Tables 1 and 2 were recalculated at the B3LYP/I optimized geometries using the basis set BSII obtained by adding to BSI polarization d- and f-functions for the main group elements[8] and Pt,[9] respectively. In order to investigate the basis set effect on the optimized geometries, we reoptimized the structures **III**, **IV**, **VI**, **VII**, **X**, **XXIIa** and **XXIV**, **XXV** (for details see below) using BSII. Symmetries of the intermediates and transition states are shown along with their structures in the figures. Normal mode analysis has been carried out only for a few transition states, as will be described in detail in the following sections. All the calculations have been performed by the Gaussian-92/DFT package,[10a] supplemented with our own ECP second-derivative routine.[10b]

At first, as a test of the reliability of the B3LYP method used throughout this paper, we have calculated the energy difference between the low-lying $^3D(s^1d^9)$ and $^1S(s^0d^{10})$ electronic states of Pt atom and the $Pt{-}BR_2$ and $Pt{-}PH_3$ binding energies of the metal-boryl $PtBR_2$ (where R = H and OH) and $Pt(PH_3)_n$ (where $n$ = 1 and 2) complexes, respectively, at the B3LYP and CCSD(T) levels of theory with the BSII. In the calculations of the $Pt{-}BR_2$ binding energies we used B3LYP/I optimized geometries of the $PtBR_2$ complexes given in Figure 1, whereas in the calculations of the $Pt{-}PH_3$ binding energies we used both the B3LYP/I and the B3LYP/II optimized geometries of the corresponding complexes in Figure 1. The results are given in the Table 1.

As seen in Table 1, for Pt atom the $^3D(s^1d^9)$ state is calculated to be the ground state, and the $^1S(s^0d^{10})$ state is 15.1 and 13.9 kcal/mol higher at the CCSD(T) and B3LYP levels, respectively, vs 11.1 kcal/mol for experiment.[11] In other words, the B3LYP/II method gives a better agreement with experiment than CCSD(T)/II and is different only by 2−3 kcal/mol from experiment. The $Pt{-}BR_2$ and $Pt{-}PH_3$ binding energies calculated at the CCSD(T)/II and B3LYP/II levels are different only up to 3.5 kcal/mol regardless the substituents on the boryl group. Therefore, one expect that the B3LYP/II//B3LYP/I approach used throughout this paper is nearly as good as CCSD(T)/II//B3LYP/II. A similar conclusion has been made in our separate paper.[2b]

However, it should be noted that the improvement of the quality of the basis sets from BSI to BSII significantly (by 0.06−0.10 Å) decreases the $Pt{-}PH_3$ bond length (from 2.22

(1) (a) Brown, H. C. *Boranes in Organic Chemistry*; Cornell University Press, London, 1972. (b) Brown, H. C. *Organic Synthesis via Organoboranes*; Wiley-Interscience: New York, 1975. (c) Pelter, A.; Smith, K.; Brown, H. C. *Borane Reagents*; Academic Press: New York, 1988. (d) Manning, D.; Noth, H. *Angew. Chem., Int. Ed. Engl.* **1985**, *24*, 878. (e) Burgess, K.; Ohlmeyer, M. J. *Chem. Rev.* **1991**, *91*, 1179 and references therein. (f) Evans, D. A.; Fu. G. C.; Hoveyda, A. H. *J. Am. Chem. Soc.* **1988**, *110*, 6917. (g) Evans, D. A.; Fu, G. C. *J. Org. Chem.* **1990**, *55*, 2280. (h) Evans, D. A.; Fu G. C. *J. Am. Chem. Soc.* **1991**, *113*, 4042. (i) Evans, D. A.; Fu G. C.; Hoveyda, A. H. *J. Am. Chem. Soc.* **1992**, *114*, 6671. (j) Evans, D. A.; Fu G. C.; Anderson, B. A. *J. Am. Chem. Soc.* **1992**, *114*, 6679. (k) Burgess, K.; Cassidy, J.; Ohlmeyer, M. J. *J. Org. Chem.* **1991**, *56*, 1020. (l) Burgess, K.; Ohlmeyer, M. J. *J. Org. Chem.* **1991**, *56*, 1027. (m) Burgess, K.; Ohlmeyer, M. J. *Tetrahedron Lett.* **1989**, *30*, 395. (n) Burgess, K.; Ohlmeyer, M. J. *Tetrahedron Lett.* **1989**, *30*, 5857. (o) Burgess, K.; Ohlmeyer, M. J. *Tetrahedron Lett.* **1989**, *30*, 5861. (p) Burgess, K.; van der Donk, W. A.; Jarstfer, M. B.; Ohlmeyer, M. J. *J. Am. Chem. Soc.* **1991**, *113*, 6139. (q) Satoh, M.; Nomoto, Y.; Miyaura, N.; Suzuki, A. *Tetrahedron Lett.* **1989**, *30*, 3789. (r) Satoh, M.; Miyaura, N.; Suzuki, A. *Tetrahedron Lett.* **1990**, *31*, 231. (s) Brown, J. M.; Lloyd-Jones, G. C. *Tetrahedron: Asym.* **1990**, *1*, 869. (t) Hayashi, T.; Matsumoto, Y.; Ito, Y. *J. Am. Chem. Soc.* **1989**, *111*, 3426. (u) Hayashi, T.; Matsumoto, Y.; Ito, Y. *Tetrahedron: Asym.* **1991**, *2*, 601. (v) Matsumoto, Y.; Hayashi, T. *Tetrahedron Lett.* **1991**, *32*, 3387. (w) Burgess, K.; Ohlmeyer, M. J. *J. Org. Chem.* **1988**, *53*, 5178. (x) Burgess, K.; van der Donk, W. A.; Ohlmeyer, M. J. *Tetrahedron: Asym.* **1991**, *2*, 613. (y) Zhang, J.; Lou, B.; Guo, G.; Dai, L. *J. Org. Chem.* **1991**, *56*, 1670. (z) Westcott, S. A.; Blom, H. P.; Marder, T. B.; Baker, R. T. *J. Am. Chem. Soc.* **1992**, *114*, 8863. (aa) Westcott, S. A.; Taylor, N. J.; Marder,T. B.; Baker, R. T.; Jones, N. J.; Calabrese, J. C. *J. Chem. Soc., Chem. Commun.* **1991**, 304. (ab) Baker, R. T.; Ovenall, D. W.; Calabrese, J. C.; Westcott, S. A.; Taylor, N. J.; Williams, I. D.; Marder, T. B. *J. Am. Chem. Soc.* **1990**, *112*, 9399. (ac) Baker, R. T.; Ovenall, D. W.; Harlow, R. L.; Westcott, S. A.; Taylor, N. J.; Marder, T. B. *Organometallics* **1990**, *9*, 3028. (ad) Westcott, S. A.; Blom, H. P.; Marder,T. B.; Baker, R. T.; Calabrese, J. C. *Inorg. Chem.* **1993**, *32*, 2175. (af) Harrison, K. N.; Marks, T. J. *J. Am. Chem. Soc.* **1992**, *114*, 9220. (ag) Burgess, K.; Jaspars, M. *Organometallics* **1993**, *12*, 497. (ah) Burgess, K.; Donk, W. A.; Kook, A. M. *J. Org. Chem.* **1991**, *56*, 2949. (ai) Knorr, J. R.; Merola, J. S. *Organometallics* **1990**, *9*, 3008. (aj) Burgess, K.; van der Donk, W. A.; Westcott, S. A.; Marder, T. B.; Baker, R. T.; Calabrese, J. C. *J. Am. Chem. Soc.* **1992**, *114*, 9350. (ak) Crabtree, R. H.; Davis, M. W. *J. Org. Chem.* **1986**, *51*, 2655. (al) Westcott, S. A.; Marder, T. B.; Baker, R. T. *Organometallics* **1993**, *12*, 975. (am) Baker, R. T.; Calabrese, J. C.; Westcott, S. A.; Nguyen, P.; Marder, T. B. *J. Am. Chem. Soc.* **1993**, *115*, 4367. (an) Hartwing, J. F.; Bhandari, S.; Rablen, P. R. *J. Am. Chem. Soc.* **1994**, *116*, 1839. (ao) Baker, R. T.; Nguyen, P.; Marder, T. B.; Westcott, S. A. *Angew. Chem., Int. Ed. Engl.* **1995,** *34*, 1336.

(2) (a) Musaev, D. G.; Mebel, A. M.; Morokuma, K. *J. Am. Chem. Soc.* **1994**, *116*, 10693. (b) Musaev, D. G.; Morokuma, K. *J. Phys. Chem.* **1996**, *100*, 6509. (c) Dorigo, A. E.; Schleyer, P. v. R. *Angew. Chem., Int. Ed. Engl.* **1995**, *34*, 878.

(3) (a) Ishiyama, T.; Nishijima, K.; Miyaura, N.; Suzuki, A. *J. Am. Chem. Soc.* **1993**, *115*, 7219 and references therein. (b) Ishiyama, T.; Matsuda, N.; Miyaura, N.; Suzuki, A. *J. Am. Chem. Soc.* **1993**, *115*, 11018. (c) Iverson, C. N.; Smith, M. R. A., III. *J. Am. Chem. Soc.* **1995,** *117*, 4403. (d) Suzuki, A. *Pure Appl. Chem.* **1994**, *66*, 213. (e) Gridnev, I. D.; Miyaura, N.; Suzuki, A. *Organometallics* **1993**, *12*, 589. (f) Lesley, G.; Nguyen, P.; Taylor, N. J.; Marder, T. B.; Scott, A. J.; Clegg, W.; Norman, N. C. *Organometallics* **1996**, *15*, 5137 and references therein. (g) Iverson, C. N.; Smith, M. R., III. *Organometallics* **1996**, *15*, 5155.

(4) For a review of boron subhalide chemistry, see: Massey, A. G. *Adv. Inorg. Chem. Radiochem.* **1983**, *26*, 1.

(5) (a) Brotherton, R. J.; McClosky, A. L.; Petterson, L. L.; Steinberg, H. *J. Am. Chem. Soc.* **1960**, *82*, 6242. (b) Welch, C. N.; Shore, S. G. *Inorg. Chem.* **1968**, *7*, 225.

(6) (a) Becke, A. D. *Phys. Rev. A* **1988**, *38*, 3098. (b) Lee, C.; Yang, W.; Parr, R. G. *Phys. Rev. B* **1988**, *37*, 785. (c) Becke, A. D. *J. Chem. Phys.* **1993**, *98*, 5648.

(7) (a) Hay, P. J.; Wadt, W. R. *J. Chem. Phys.* **1985**, 82, 299. (b) Wadt, W. R.; Hay, P. J. *J. Chem. Phys.* **1985**, *82*, 284.

(8) (a) Dunning, T. M., Jr. *J. Chem. Phys.* **1971**, *55*, 716. (b) Dunning, T. M., Jr. *J. Chem. Phys.* **1970**, *53*, 2823.

(9) Ehlers, A. W.; Böhme, M.; Dapprich, S.; Gobbi, A.; Höllwarth, A.; Jonas, V.; Köhler, K. F.; Stegmann, R.; Veldkamp, A.; and Frenking, G. *Chem. Phys. Lett.* **1993**, *208*, 111.

(10) (a) Frisch, M. J.; Trucks, G. W.; Head-Gordon, M.; Gill, P. M. W.; Wong, M. W.; Foresman, J. B.; Johnson, B. G.; Schlegel, H. B.; Robb, M. A.; Replogle, E. S.; Gomperts, R.; Andres, J. L.; Raghavachari, K.; Binkley, J. S.; Gonzales, C.; Martin, R. L.; Fox, D. J.; DeFrees, D. J.; Baker, J.; Stewart, J. J. P.; Pople, J. A. *GAUSSIAN 92/DFT*; Gaussian Inc.: Pittsburgh, PA, 1992. (b) Cui, Q.; Musaev, D. G.; Svensson, M.; Morokuma, K. *J. Phys. Chem.* **1996**, *100*, 10936.

(11) Moore, C. F. *Atomic Energy Levels*, NSRD-NBS; U.S. Goverment Printing Office: Washington, DC, 1971; Vol. III.

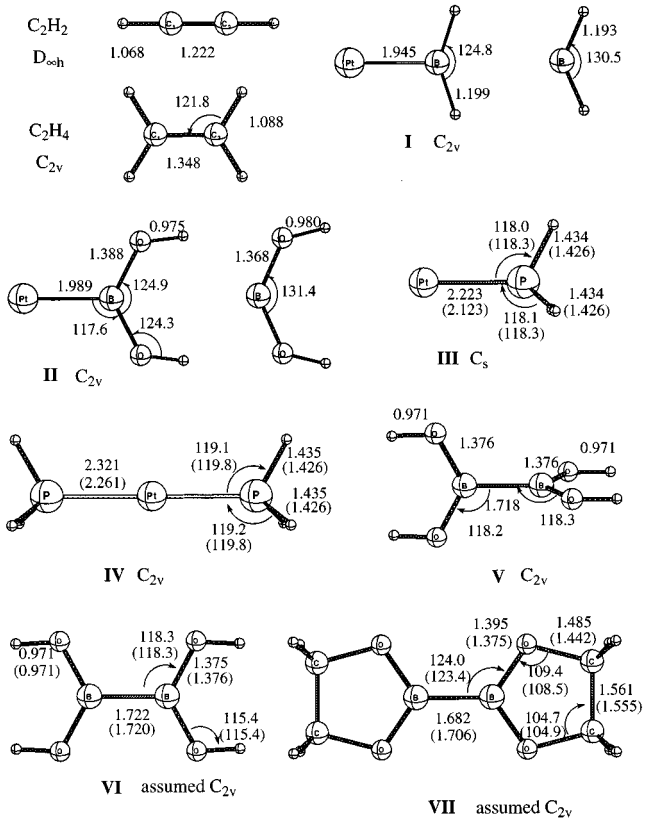


**Figure 1.** B3LYP/I optimized geometries (in Å and deg) of the $PtBR_2$ complex, $BR_2$ (where R = OH and H), and the reactants $PtPH_3$, $Pt(PH_3)_2$, $[B(OH)_2]_2$, and $[B(OCH_2)_2]_2$. Numbers in the parentheses are obtained by adding the polarization function on elements excluding Pt and H.

**Table 1. Relative Energies (in kcal/mol) of Two States of the Pt Atom and the Pt−B and Pt−P Binding Energies (in kcal/mol) at the B3LYP/II and CCSD(T)/II level at B3LYP/I Optimized Geometries[a]**

| | state | CCSD(T)/II | B3LYP/II | expt |
|---|---|---|---|---|
| Pt | $^3D$, $s^1d^9$ | 0.0 | 0.0 | 0.0 |
| | $^1S$, $s^0d^{10}$ | 15.1 | 13.9 | 11.1 |
| $PtBH_2$, **I** | $^2A_1$ | 93.3 | 96.8 | |
| $PtB(OH)_2$, **II** | $^2A_1$ | 91.0 | 89.1 | |
| $PtPH_3$, **III** | $^1A'$ | 51.7 | 54.6 (56.6)[b] | |
| $Pt(PH_3)_2$, **IV** | $^1A_1$ | 41.4 | 38.9 (38.3)[b] | |

[a] Total energy of $BR_2$ is −25.817 789 and −25.935 421 au for R = H, and −176.066 975 and −176.547 552 au for R = OH at the CCSD(T)/II and B3LYP/II levels, respectively. Total energy of $PH_3$ is −8.210 04 and −8.301 62 au at the CCSD(T)/II and B3LYP/II levels, respectively. No zero point energy is included. [b] At the B3LYP/II optimized geometry.

and 2.32 Å, at the B3LYP/I level, to 2.12 and 2.26 Å at the B3LYP/II level, for the singlet $PtPH_3$ and $Pt(PH_3)_2$ complexes, respectively, as shown in Figure 1), while it only slightly affects other geometrical parameters and the $Pt-PH_3$ binding energies. These results are also in good agreement with previous studies.[12a]

In order to justify the models used in this paper we also have studied the structure and stability of $B_2[(OH)_2]_2$ and $B_2[(OCH_2)_2]$. The global minimum of the model compound $B_2[(OH)_2]_2$ is calculated to be structure **V** in Figure 1with two $B(OH)_2$ groups perpendicular to each other. The structure **VI** with coplanar $B(OH)_2$ groups lies only 0.6 kcal/mol higher. Since the latter can interact more strongly with the metal center than the former via back-donation from the metal $d_\sigma$ orbital, we will use only the structure **VI** with coplanar $B(OH)_2$ groups in the following discussions. The calculated B−B and B−O bond lengths in the model $B_2[(OH)_2]_2$, **VI**, are 1.722 and 1.375 Å, vs 1.682 and 1.395 Å, respectively, in the experimentally used $B_2[(OCH_2)_2]_2$, **VII**. These calculated numbers are in good agreement with 1.678 ± 0.003 and 1.388 ± 0.003 Å, respectively, measured experimentally for $B_2(4\text{-}t\text{-Bu-cat})_2$.[3f] The use of the larger BSII basis set only slightly changes the geometries of **V**−**VII**. These results once again confirm the reliability of the B3LYP/II//B3LYP/I method used in this paper. In addition, the similarity in the calculated B−B and B−O bond lengths and in the calculated B−B binding energies, 106.2 and 109.6 kcal/mol, between the model $B_2[(OH)_2]_2$ and the real $B_2[(OCH_2)_2]_2$ molecules indicates that $B_2[(OH)_2]_2$ is an electronically adequate model of $B_2pin_2$ used by experimentalists.

With the above discussion, we believe that the results obtained in this work are reliable for the discussion of mechanism of the actual catalytic cycle. In the following sections, geometries of the reactants, transition states, intermediates, and products of the reactions 1 and 2 are obtained mainly at the B3LYP/I level, while energetics are calculated at the B3LYP/II//B3LYP/I level.

**Scheme 1. Proposed Mechanism of Alkyne and Alkene Diboration by the $Pt(PR_3)_2$ Catalyst**

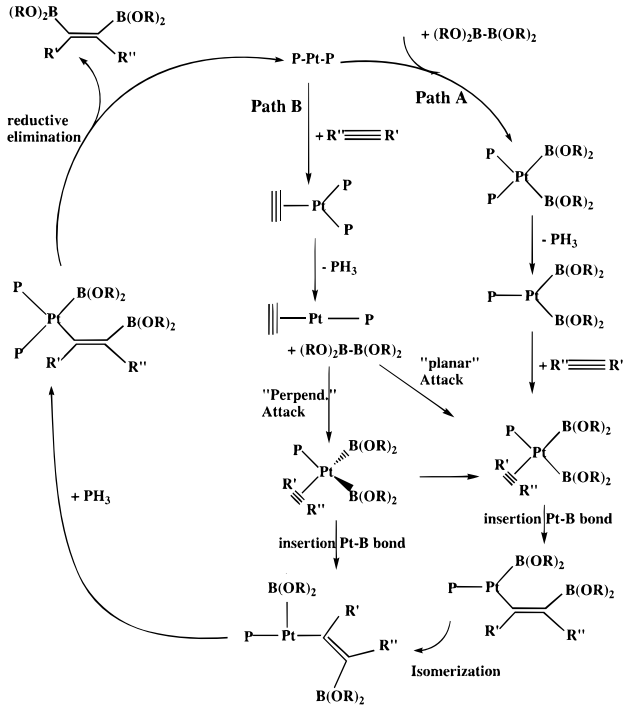


## III. Mechanism of Reactions 1 and 2

The proposed mechanism, shown in Scheme 1, includes two paths, A and B. In path A the first step is the coordination of $R_2B-BR_2$ to $Pt(PH_3)_2$, while in path B the first step is the coordination of acetylene/ethylene to $Pt(PH_3)_2$. In this section, we will discuss the path A in detail. The preliminary results for path B will be discussed in the subsequent section.

As seen in Scheme 1, at the beginning the reactions 1 and 2 proceed via same intermediates and transition

(12) Musaev, D. G.; Morokuma, K. *Adv. Chem. Phys. Vol. XCV*; Progogine, I., Rice S. A., Eds.; John Wiley & Sons, Inc.: New York, 1996; p 61−127 and references therein. (b) Yoshida, S.; Sakaki, S.; Kobayashi, H. *Electronic Processes in Catalyst*; VCH: Weinheim, Germany, 1994; and references therein.

(13) Nguyen, P.; Dai, C.; Taylor, N. J.; Power, W. P.; Marder, T. B.; Pickett, N. L.; Norman, N. C. *Inorg. Chem.* **1995**, *34*, 4290.

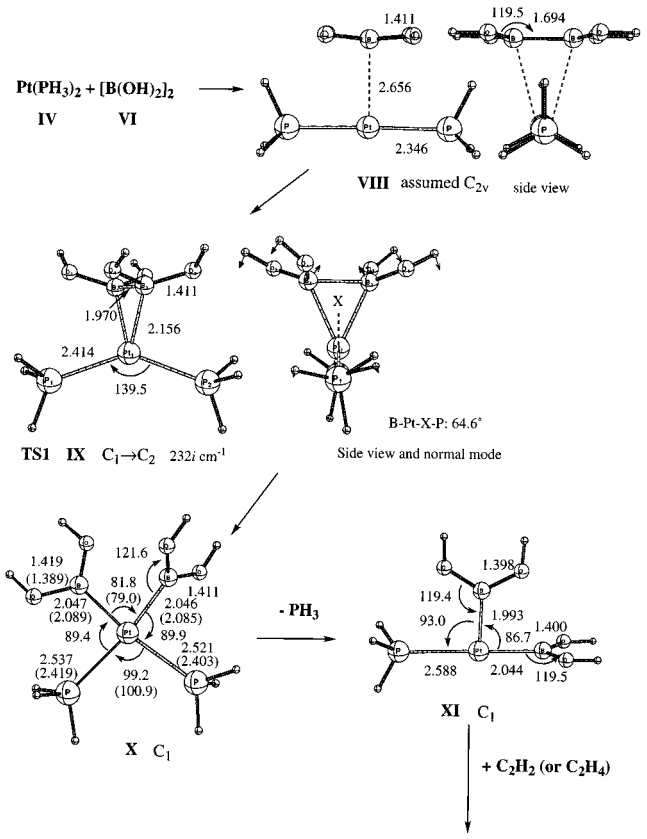


**Figure 2.** B3LYP/I optimized geometries (in Å and deg) of the intermediates and transition states of the initial steps in path A. Numbers in the parentheses are obtained by adding the polarization function on elements excluding Pt and H. The arrows on **IX** show the reaction coordinate vector.

states. The first step is the coordination of $(OH)_2B-B(OH)_2$ to $Pt(PH_3)_2$ to give a molecular complex **VIII**, shown in Figure 2, where the B−B and P−Pt−P axes are perpendicular to each other and the B−B bond is only 0.008 Å shorter, the Pt−P bond is 0.025 Å longer, and the P−Pt−P angle is 1.5° smaller than those in the free $(OH)_2B-B(OH)_2$ and $Pt(PH_3)_2$ species, respectively. The Pt−B bond distance and the $(OH)_2B-B(OH)_2$ + $Pt(PH_3)_2$ complexation energy is calculated to be 2.656 Å and 3.7 kcal/mol, respectively, as shown in Table 2. The molecular complex with the B−B axis parallel to P−Pt−P was not found, which would be unfavorable due to steric repulsion.

The next step is the activation of the B−B bond, and it takes place through transition state **IX** in Figure 2, where the B−B, Pt−B, and Pt−P bonds, 1.970, 2.156, and 2.414 Å, respectively, are 0.276 Å longer, 0.500 Å shorter, and 0.068 Å longer than those in the molecular complex **VIII**. The P−Pt−P angle is reduced from 180.0 to 139.5°. It is interesting to note that B−Pt−B plane rotates with respect to P−Pt−P plane as the reaction goes from molecular complex $(R_2B-BR_2)Pt(PH_3)_2$, **VIII**, to oxidative addition product $(R_2B)(BR_2)Pt(PH_3)_2$, **X**. At the transition state **IX**, the dihedral angle BPtPP is defined to be 64.6° (with 180° corresponding to square planar structure and 90° to perpendicular orientation of B−Pt−B with respect to P−Pt−P). The activation barrier is calculated to be 8.8 and 12.5 kcal/mol relative to the reactants and the molecular complex **VIII**, respectively, as shown in Table 2.

**Table 2. Total Energy (in au, in Italics) of Reference Systems and Relative Energies (in kcal/mol), Relative to $Pt(PH_3)_2 + [B(OH)_2]_2 + C_2H_x$, of Intermediates and Transition States at the B3LYP/II Level at B3LYP/I Optimized Geometries[a]**

| compd | $C_2H_2$ | $C_2H_4$ |
|---|---|---|
| $Pt(PH_3)_2$, **IV** | *−135.8314* | |
| $B_2(O_2H_2)_2$, **VI** | *−353.2644* | |
| $B_2(C_2O_2H_4)_2$, **VII** | *−508.0924* | |
| $C_2H_x$ | *−77.3307* | *−78.5946* |
| $PH_3$ | *−8.3016* | |
| path A **VIII** | −3.7 | |
| TS1, **IX** | 8.8 | |
| **X** | −10.9 (−10.1)[b] | |
| **XXV** | (−12.4) | |
| **XI** | 7.9 | |
| **XIIa/o** | −5.0 | −7.0 |
| TS2, **XIIIa/o** | 4.0 | 15.9 |
| **XIVa/o** | −33.1 | −2.9 |
| TS3, **XVa/o** | −19.1 | 9.4 |
| **XVIa/o** | −50.3 | −21.8 |
| **XVIIa/o** | −54.4 [−55.2][c] | −26.8 |
| TS4, **XVIIIa/o** | −42.0 [−46.1] | −12.8 |
| **XIXa/o** | −73.2 | |
| products, **XXa/o** | −60.8 [−68.3] | −41.7 |
| path B **XXIIa/o** | −17.7 (−17.5) | −12.5 |
| **XXIVa/o** | (−11.6) | (−6.9) |
| **XXVIa/o** | 1.1 (1.8) | 3.8 |

[a] No zero point energy is included. [b] Numbers in parentheses are at the B3LYP/II geometry. [c] Numbers in brackets are for the *trans* structures.

Overcoming the transition state **IX** leads to the oxidative addition product, **X**, where the $B(OH)_2$ fragments are positioned *cis* to each other, and the OBO planes are mutually perpendicular to avoid steric repulsion. As seen in Figure 2, the two sets of Pt−P and Pt−B bond lengths differ by a few hundredths of an angstrom, and the average values will be used in the following discussions. The Pt−P bond in the oxidative addition product, **X**, is significantly stretched, from 2.321 Å in free $Pt(PH_3)_2$ to 2.537 Å. The comparison of the calculated geometries of the structure **X** with those from X-ray experiment for *cis*-$[(PPh_3)_2Pt(Bcat)_2]$[3e] shows excellent agreement for the Pt−B bond length; the calculated 2.046 Å is very close to the experimentally measured, 2.049(6) Å. However, the agreement between experimental and calculated bond angles is not as good for bond lengths: The calculated P−Pt−P and B−Pt−B angles in **X** are 99.2 and 81.8° vs 108.1 and 77.1° in the experiment, respectively. We also find a large, 0.17 Å, discrepancy between experimental, 2.35 Å, and calculated, 2.537 Å, Pt−P bond lengths, which can be attributed to the absence of a polarization d-function for the P atoms in the BSI used in geometry optimization. Indeed, as seen in Figure 2, the Pt−P bond length calculated at the B3LYP/II level, 2.419 Å, is in much better agreement with the experiment.[3e] One should note that using B3LYP/II for geometry optimization does not change significantly either other geometrical parameters or the relative energies.

The following steps are dissociation of $PH_3$ from **X** and coordination of acetylene or ethylene. The dissociation of one of the $PH_3$ ligands from **X** leads to the unsaturated three-coordinate complex $(PH_3)Pt(BR_2)_2$ **XI** with well-defined T-shape structure where the Pt−B bond *trans* to the open site shortens to 1.993 Å from 2.047 Å in **X**, while the one *cis* to the open site is nearly unchanged. Though these two steps can, in principle,

take place in an associative fashion by addition of $C_2H_x$ ($x = 2,4$) followed by dissociation of $PH_3$, via a five-coordinate complex. However, no five-coordinate complex was found in the calculation, and we conclude that this process takes place only in a dissociative fashion. This result has been confirmed by a recent experiment[3g] published while our manuscript was being reviewed; Iverson and Smith have found that the stoichiometric results exclude simple, bimolecular insertion of an alkyne into Pt−B bonds of $(Ph_3P)_2Pt(Bcat)_2$ and that the observed dependence on phosphine and alkyne strongly favors a mechanism where phosphine dissociation generates a three-coordinate intermediate that mediates alkyne insertion.

The $PH_3$ dissociation energy from **X** to **XI** is calculated to be 18.8 kcal/mol which is much smaller than the binding energy of $PH_3$ to bare Pt, 54.6 kcal/mol, and to $Pt(PH_3)$, 38.9 kcal/mol. Following the dissociation of $PH_3$, one acetylene or alkene molecule coordinates to **XI** at the open site to form structure **XIIa** or **XIIo** (**a** stands for acetylene and **o** for ethylene). Since the geometries and energetics of the intermediates and transition states for the reactions 1 and 2 should be different starting from structures **XIIa** and **XIIo**, we will examine them separately for acetylene and ethylene.

**$C_2H_2$.** The complex **XIIa** is rather floppy; the $C_2H_2$ ligand rotates nearly freely around the Pt−X axis, X being the center of the C−C bond, with a barrier of less than 1 kcal/mol. Therefore, the structure **XIIa** shown in Figure 3 is optimized with the constraint that C−C−Pt−P is coplanar. The calculated Pt−C distance in **XIIa** is rather long, 2.300 Å, compared with that in a metallacycle (∼2.1 Å), while the C−C bond is close to that in the free molecule $C_2H_2$, showing that **XIIa** is a $\pi$-complex. Forcing the C−C bond to be perpendicular to the P−Pt−B plane results in a structure with an even longer Pt−C bond, ∼2.4 Å, while the energy is nearly the same as **XIIa**. The coordination energy of $C_2H_2$ to **XI** is calculated to be 13.0 kcal/mol. Thus, **XIIa** lies 5.0 kcal/mol lower than the reactants, $Pt(PH_3)_2 + [B(OH)_2]_2 + C_2H_2$.

Starting from complex **XIIa**, the next step of the reaction is the insertion of $C_2H_2$ into the Pt−B bond via the transition state **XIIIa**, which leads to an intermediate **XIVa**. In **XIVa** one of the carbon atoms forms a $\sigma$ bond with the metal with a distance of 2.125 Å, and the other forms a B−C bond with a distance of 1.531 Å. As a result the Pt−B and the C−C $\pi$ bonds are broken. The $B(OH)_2$ group rotates around the B−C bond so that an oxygen atom can interact with the open site of the metal center. Consequently, the length of this interacting O−B bond is stretched to 1.438 Å, compared with 1.379 Å of the O−B pointing away from the metal. The Pt−P bond is shortened from 2.516 Å in **XIIa** to 2.277 Å in **XIVa**, obviously due to the loss of strong *trans* influence. The insertion process is calculated to be exothermic by 28.1 kcal/mol.

The transition state for the insertion of $C_2H_2$ into the Pt−B bond, **XIIIa**, was optimized with $C_s$ symmetry constraint. The $C_2H_2$ group is much closer to the metal in **XIIIa** with the Pt−C bonds of 2.112 and 2.243 Å than in complex **XIIa**. The C−C bond is stretched from 1.254 Å in **XIIa** to 1.321 Å, and the H−C−C angles decrease from 160 to ∼133°, clearly showing the change of

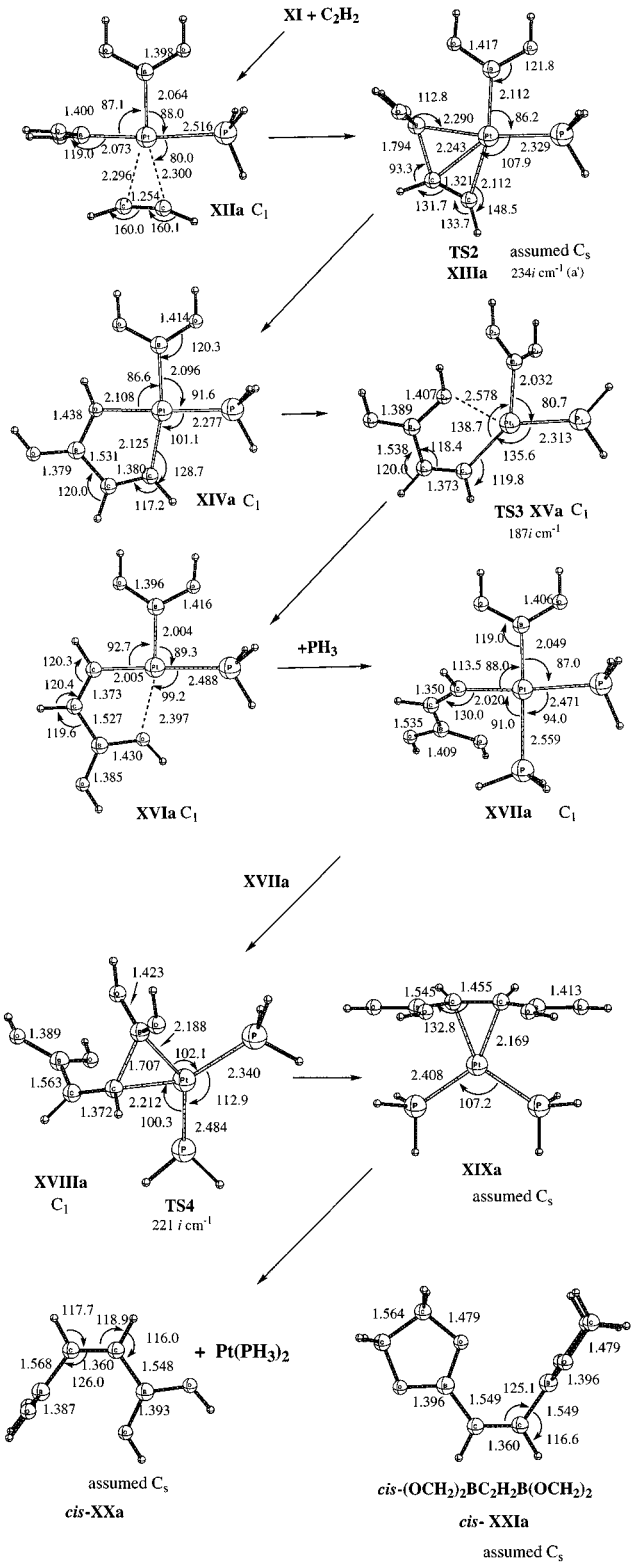


**Figure 3.** B3LYP/I optimized geometries (in Å and deg) of the intermediates and transition states of the final steps in path A of acetylene reaction 1.

hybridization of the carbon atoms to $sp^2$. The forming C−B bond in **XIIIa** is 1.794 Å vs 1.438 Å in product **XIVa**, while the breaking Pt−B bond, 2.290 Å, is 0.22 Å longer than in complex **XIIa**. Normal mode analysis shows that the structure **XIIIa** has two imaginary frequencies. The frequency 234*i* $cm^{-1}$ in a′ represents the reaction coordinate, while the very small frequency 55*i* $cm^{-1}$ in a″ corresponds to out-of-plane rotation of the reacting $B(OH)_2$ group. As discussed above, this

$B(OH)_2$ group will rotate to occupy the empty site of the metal in **XIVa**, and it is not surprising that the true saddle point wants to adopt $C_1$ symmetry. However, the imaginary frequency is so small that the energy of **XIIIa** is expected to be very close to that of the true saddle point. Thus we did not search for the TS without symmetry. The barrier height at **XIIIa** measured from **XIIa** is 9.0 kcal/mol.

From **XIVa** the mechanism of reaction could be very complex. The second $B(OH)_2$ and the $CH{=}CH[B(OH)_2]$ ligands are *trans* to each other in **XIVa** and cannot directly form a bond in a in-plane reaction. One can consider two possible pathways. The first is that both ligands bend up from the planar position toward each other and the C-B bond is formed directly through a tetrahedral transition state. It is well−known that tetrahedral structures for $d^{10}$ complexes are very unstable,[14] thus we did not examine this path. The second is the in-plane isomerization of *trans* complex **XIVa** to a *cis* complex **XVIa**. This process from **XIVa** to **XVIa** is exothermic by 17.2 kcal/mol. The reason why **XVIa** is more stable than **XIVa** is clear by considering the arrangement of strong donating ligands; the two strong $\sigma$ ligands $B(OH)_2$ and $CH{=}CH[B(OH)_2]$ are *trans* to each other in **XIVa** and *cis* to each other in **XVIa**. Thus the Pt−B and Pt−C bonds in **XIVa** are weaker than those in **XVIa**, as clearly seen from the bond distances. For example, the Pt−C bond is 2.13 Å in **XIVa** but only 2.01 Å in **XVIa**. The optimized isomerization transition state **XVa** has the expected Y-shape as shown in Figure 3. It is interesting to note that the $CH{=}CHB(OH)_2$ group also rotates around the Pt−C bond to avoid the repulsion with the $B(OH)_2$ ligand and to retain the energy of coordination to the metal at the O end, with the B−Pt−C=C dihedral angle of −50.4° at TS **XVa**. As the $CH{=}CH[B(OH)_2]$ ligand moves from *trans* to *cis* position, the B−Pt−P angle of 92° in **XIVa** decreases to 81° at the TS **XVa** and then increases back to 90° in the product **XVIa**. Normal mode analysis confirms that this structure has one imaginary frequency, $187i$ $cm^{-1}$. The isomerization barrier height, 14.0 kcal/mol, is substantial despite the large exothermicity from **XIVa** to **XVIa**. Note that this isomerization step is completely ignored in the previous study of silastannation of alkynes with Pd catalyst.[15]

Next recoordination of $PH_3$ to **XVIa** without barrier leads to the complex **XVIIa**. The complex **XVIIa** has a square planar structure similar to **X**. The Pt−P bond *trans* to $B(OH)_2$, 2.559 Å, is longer than that *trans* to $CH{=}CHB(OH)_2$, 2.471 Å, reflecting the weaker *trans* influence of the latter as was discussed for **XIVa** and **XVIa** above. The B−Pt−C=C dihedral angle is 121.1°, indicating the $CB(OH)_2$ part is out of plane from the nearly square-coplanar Pt and P−P−B−C backbone. There is another structure for complex **XVIIa**, in which Pt and $B(OH)_2$ are *trans* with respect to the C=C bond. As shown in Table 2, this structure is actually 0.8 kcal/mol more stable than the *cis* structure. However, a high barrier of rotation would be required to reach the *trans* isomer and this isomerization is not likely to take place.

The binding energy of $PH_3$ from **XVIa** to **XVIIa** is only 4.1 kcal/mol, as we lose the interaction between Pt and O in **XVIIa**. However, it should be noted that recoordination of this second $PH_3$ ligand is definitely needed to stabilize the following reductive elimination process, to avoid a highly unsaturated intermediate. The combined process from **XIVa** to **XVIIa** is 21.3 kcal/mol exothermic.

From **XVIIa** the reductive elimination of *cis*-$B(OH)_2CH{=}CHB(OH)_2$ product takes place through the transition state **XVIIIa**. At TS **XVIIIa**, the B−C bond is being formed, 1.707 Å vs 1.568 Å in the product **XXa**, and the Pt−B and Pt−C bonds are being broken, from 2.049 and 2.020 Å in **XVIIa** to 2.188, and 2.212 Å, respectively, in **XVIIIa**. The P−Pt−P angle is opened to 112.9°, on the way to the product complex **XIXa**. Normal mode analysis has confirmed that **XVIIIa** is a real saddle point, with an imaginary frequency of $221i$ $cm^{-1}$. The elimination barrier is calculated to be 12.4 kcal/mol relative to complex **XVIIIa**.

The product complex, **XIXa**, is typical for a $\pi$ complex, with Pt−C distance of 2.16 Å. The binding energy of **XIXa** relative to the final products *cis*-$B(OH)_2CH{=}CHB(OH)_2$ and $Pt(PH_3)_2$ is calculated to be 12.4 kcal/mol. The entire reaction 1, which is nothing but the reaction of $CH{\equiv}CH$ and $[B(OH)_2]_2$ to form *cis*-$B(OH)_2CH{=}CHB(OH)_2$, is exothermic by 60.8 kcal/mol.

In order to verify how real the adopted model reactant $[B(OH)_2]_2$ is, as well as to test the present method once again, we carried out calculations for the product of reaction 1 with the more realistic model reactant $B_2[(OCH_2)_2]_2$. The optimized structure of the product **XXIa** is shown also in Figure 3. The calculated geometrical parameters of **XXIa** agree well with the experimental X-ray results obtained for (*E*)-(4-$MeOC_6H_4$)C(Bcat)=CH(Bcat).[3f] The calculated C−C and C-B bond distances are 1.360 and 1.549 Å vs experimental 1.348 ± 0.002 and 1.526 ± 0.002 Å, respectively, and the calculated B−C−C bond angle is 125.1° vs experimental 124.4 ± 0.1°. The exothermicity of the overall reaction for $B_2[(OCH_2)_2]_2$ is calculated to be 56.1 kcal/mol, similar to the above 60.8 kcal/mol for $B_2[(OH)_2]_2$, once again confirming that $B_2[(OH)_2]_2$ is a reasonable model for simulating the real catalytic reaction with $B_2cat_2$.

In the above paragraphs, we have seen that the mechanism for alkyne diboration requires the *cis* stereochemistry to be maintained for the intermediate complexes and final products. *Trans*-isomers cannot be produced because the required isomerization around the C=C double bond is energetically prohibitive. This is consistent with the experiment,[3f] in which only *cis* isomers are obtained.

**$C_2H_4$.** For the current reaction involving $C_2H_4$, we followed the same mechanism as discussed in the case of $C_2H_2$. After the oxidative addition of B−B to $Pt(PH_3)_2$ and dissociation of $PH_3$, the olefin can coordinate to **XI** to give complex **XIIo**. The coordination energy is calculated to be 14.9 kcal/mol, about 2 kcal/mol larger than in **XIIa**. The $C_2H_4$ group can easily (with less than 1 kcal/mol barrier) rotate around the Pt−X axis, X being the center of the C−C bond. The structure **XIIo** shown in Figure 4 is optimized with the constraint that C−C−Pt−P is coplanar, as in the case of acetylene. The Pt−C and C−C distances are calculated to be 2.38−2.40 and

(14) Yamamoto, A. *Organotransition Metal Chemistry*; John Wiley & Sons: New York, 1986.

(15) Hada, M.; Tanaka, Y.; Ito, M.; Murakami, M.; Amii, H.; Ito, Y.; Nakatsuji, H. *J. Am. Chem. Soc.* **1994**, *116*, 8754.

(16) Cui, Q.; Musaev, D. G.; Morokuma, K. To be submitted for publication.

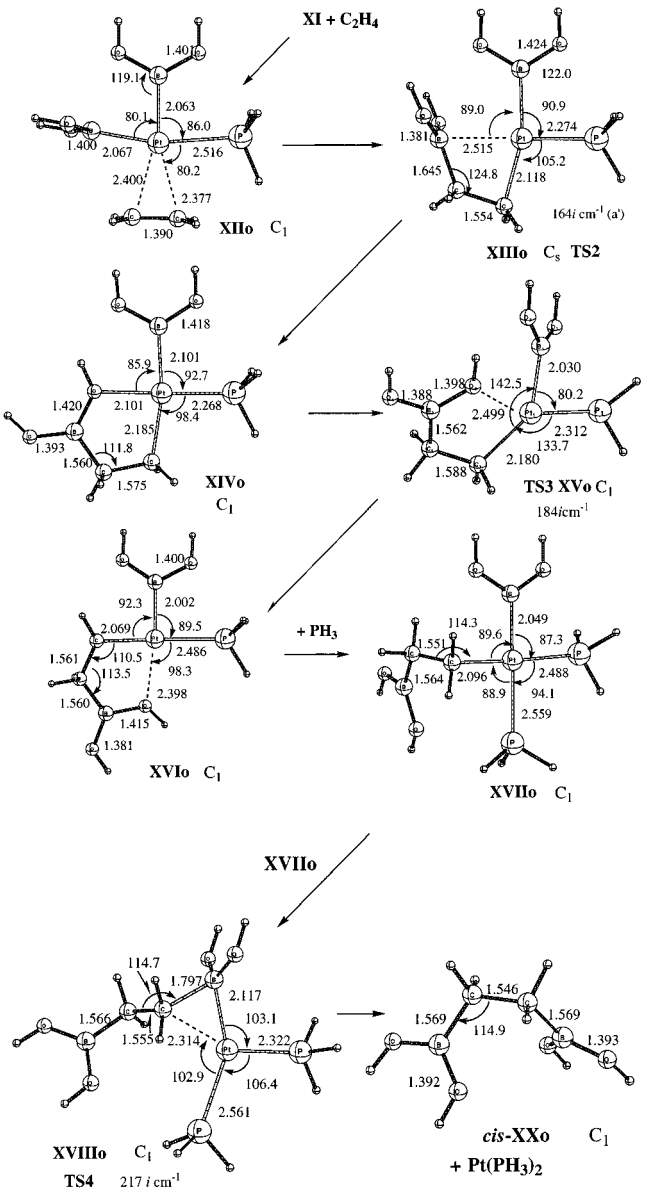


**Figure 4.** B3LYP/I optimized geometries (in Å and deg) of the intermediates and transition states of the final steps in path A of ethylene reaction 2.

1.390 Å, respectively, the former being about 0.09 Å longer than in **XIIa**. **XIIo** lies 7.0 kcal/mol lower than the reactants, $Pt(PH_3)_2 + [B(OH)_2]_2 + C_2H_4$.

Starting from complex **XIIo** the next step of reaction is the insertion of $C_2H_4$ into the Pt−B bond, which takes place through TS **XIIIo** and leads to intermediate **XIVo** where one of the C atoms forms a $\sigma$ bond with Pt with a distance of 2.185 Å and the other forms the C-B bond with a distance of 1.560 Å. The $B(OH)_2$ group rotates around the C-B bond so that an oxygen atom can interact with the open site of the metal center. Consequently, the interacting O−B bond length is stretched to 1.420 Å, compared with 1.393 Å of the O−B bond pointing away from the metal. The P−Pt bond is shortened from 2.516 Å in **XIIo** to 2.268 Å in **XIVo**. The insertion process is calculated to be endothermic by 4.1 kcal/mol. The transition state corresponding to the insertion of $C_2H_4$ into the Pt−B bond, **XIIIo,** has $C_s$ symmetry with the Pt−C and Pt−B bonds of 2.118 and 2.515 Å, respectively. The length of the C−B bond being formed is 1.645 Å. Normal mode analysis shows that the structure has one imaginary frequency, $164i$ $cm^{-1}$, in a′. The barrier height from **XIIo** is calculated to be 22.9 kcal/mol.

The next step of reaction should be the isomerization of complex **XIVo** (where the $CH_2CH_2B(OH)_2$ and $B(OH)_2$ ligands are *trans* to each other) to complex **XVIo** (where the $CH_2CH_2B(OH)_2$ and $B(OH)_2$ ligands are *cis* to each other) via transition state **XVo**. The *cis*-complex **XVIo** is calculated to be 18.9 kcal/mol lower than *trans*-complex **XIVo**. The isomerization transition state, **XVo**, adopting a Y-shaped structure, is calculated to be 12.3 kcal/mol higher than **XIVo**. After the isomerization the coordination of the second $PH_3$ ligand to the Pt center of **XVIo** takes place without barrier and leads to complex **XVIIo**. The entire process from **XIVo** leading to **XVIIo** is 23.9 kcal/mol exothermic.

From **XVIIo** the elimination of *cis*-$B(OH)_2CH_2CH_2B(OH)_2$ product takes place through the transition state **XVIIIo** to the product **XIXo**. In TS **XVIIIo** the B−C bond being formed is 1.797 Å vs 1.569 Å in the product **XVIXo**, and the Pt−B bond is being stretched from 2.049 Å in **XVIIa** to 2.117 Å. Normal mode analysis confirms that **XVIIIo** is a real transition state, with an imaginary frequency of $217i$ $cm^{-1}$. The elimination barrier is calculated to be 14.0 kcal/mol relative to complex **XVIIa**. In principle, there should be a weakly bound complex between the product $B(OH)_2CH_2CH_2B(OH)_2$ and $Pt(PH_3)_2$, resembling **XIXa** in the case of $C_2H_2$. However, the interaction is expected to be much weaker, with a magnitude of ∼5 kcal/mol, because the product only contains single bonds. Thus we did not locate this complex. The entire reaction 2 is exothermic by 41.7 kcal/mol.

## IV. Mechanism of Reaction for Path B: a Preliminary Study

Aside from the path A explored above, we also investigated another possible branch of the catalytic cycle, path B in Scheme 1. In this path, acetylene/ethylene coordination taking place as the first step. It is well−known that for metal centers with $d^{10}$ configuration, acetylene and ethylene prefer to coordinate in a coplanar fashion.[15] Therefore we calculated only coplanar coordination of $C_2H_2$ and $C_2H_4$ to the metal center. As seen in Figure 5, $C_2H_2$ and $C_2H_4$ coordinate to $Pt(PH_3)_2$ to give the metallacycle complex **XXIIa** and **XXIIo**, respectively. The calculated Pt−C bond distances are 2.075 and 2.132 Å for $C_2H_2$ and $C_2H_4$, respectively. The C−C bond distances are 1.304 and 1.451 Å for $C_2H_2$ and $C_2H_4$ and are 0.08 and 0.10 Å longer than that in the free molecules, respectively. The coordination energies of $C_2H_2$ and $C_2H_4$ to $Pt(PH_3)_2$, 17.7 and 12.5 kcal/mol, respectively, are much smaller than a typical energy of formation, ∼40 kcal/mol, for a strong metallacycle.[12] Upon $C_2H_x$ coordination, the metal−$PH_3$ bond is weakened, as reflected in the stretched (∼0.1 Å) Pt−P distances and the opened P−Pt−P angle. The cost of these structural changes must make the net coordination energy of $C_2H_x$ smaller than that for typical metallacycles. The calculated coordination energy of acetylene and ethylene to $Pt(PH_3)_2$, 17.7 and 12.5 kcal/mol, respectively, is 7 and 2 kcal/mol larger than the energy of oxidative addition of $(OH)_2B−B(OH)_2$ to $Pt(PH_3)_2$, 10.9 kcal/mol in path A. This result is contradictory to the experimental findings of Iverson

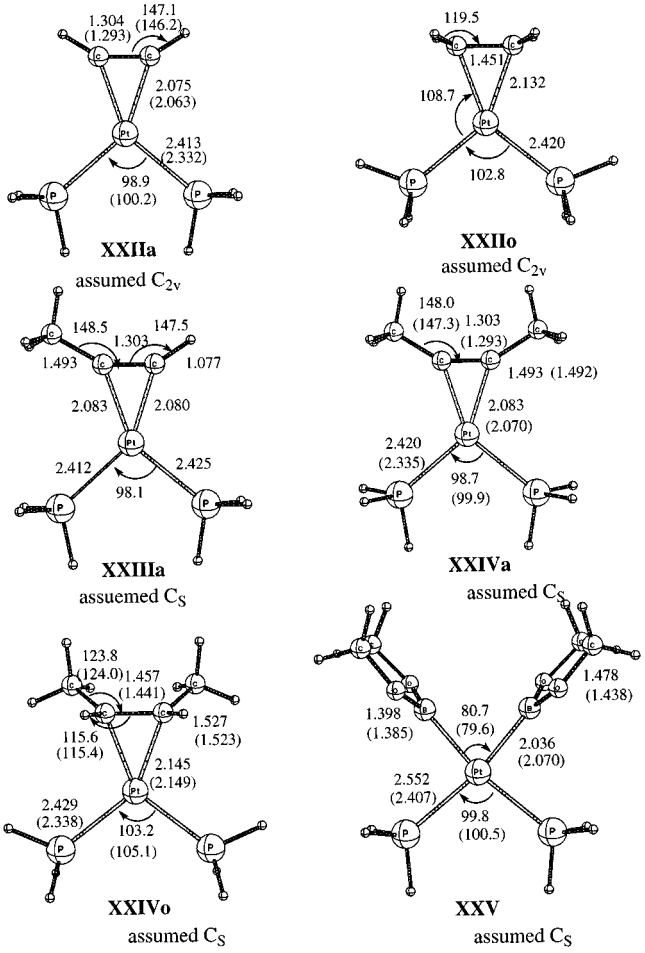


**Figure 5.** B3LYP/I optimized geometries (in Å and deg) of the complexes formed between alkyne, alkene, and $(OH)_2B-B(OH)_2$ in the initial step of path B. Numbers in the parentheses are obtained by adding the polarization function on elements excluding Pt and H.

and Smith,[3c] who have shown that alkyne complex $[(PPh_3)_2Pt(\eta^2\text{-4-octyne})]$ reacts with $B_2cat_2$ and generates the B−B oxidative addition complex, with loss of alkyne. In order to explain this difference between experiment and calculations, we should recall the fact that the binding energy of alkynes to transition metal decreases as the size of the alkyne increases. As an example, we have calculated the binding energies of $C_2HMe$, $C_2Me_2$, and $C_2H_2Me_2$ to $Pt(PH_3)_2$. The optimized structures are denoted as **XXIIIa** and **XXIVa/o** in Figure 5. The binding energy of alkynes drops from 17.7 kcal/mol in $C_2H_2$ case to 12.6 and 11.6 kcal/mol in $C_2HMe$ and $C_2Me_2$, respectively. Similarly, the binding energy of alkene drops from 12.6 kcal/mol for $C_2H_4$ to 6.9 kcal/mol for $C_2H_2Me_2$. The binding energy of B−B, on the other hand, increases as the substituent size increases. As an illustration, we have calculated the binding energy of B−B for $B_2[(OH)_2]_2$. The binding energy of the B−B group in the oxidative addition product **XXV** is 12.4 kcal/mol at the B3LYP/BSII level. Thus, the binding energy of $B_2[(OH)_2]_2$ is larger than that of substituted acetylene and ethylene used in the experiments, which makes path A more favorable for substituent alkynes. We believe at this stage that the coordination of substituted alkynes (or alkenes) is very unlikely to be the initial step in the real Pt(0)-catalyzed alkyne (or alkene) diboration reaction. A more detailed study of path B will be presented separately in our upcoming paper.[16]

## V. Comparison of Acetylene and Ethylene Diboration

The overall potential energy profiles of the path A of the entire catalytic cycle for acetylene and ethylene diboration reactions 1 and 2 are shown in Figure 6. As seen from the figure, the two most important steps of the alkyne diboration reaction on Pt(0) complex are the B−B activation and $PH_3$ dissociation from **X**. Reductive elimination is less energetically demanding compared to the above two steps. With the present level of theory, B3LYP/II//B3LYP/I, $PH_3$ dissociation is energetically more demanding than B−B activation, which takes place with a 18.8 kcal/mol energy vs 14.0 kcal/mol for B−B activation. In addition, the three-coordinate complex $(PH_3)Pt(BR_2)_2$, **XI**, is highly unsaturated; thus, the competition between the coordination of $PH_3$ and $C_2H_2$ is crucial to the catalytic efficiency. Indeed, the argument that $PH_3$ dissociation is the rate-determining step in the entire catalytic cycle is strongly supported by experimental findings.[3a,b,d,f] It is found in the experiment that addition of $PPh_3$ or the presence of a more strongly binding bidentate phosphine actually inhibits the reaction.[3f] In a comparison of the endothermicity of the $PH_3$ dissociation from the B−B oxidative addition product **X** (18.8 kcal/mol) with that from reactant $Pt(PH_3)_2$ (38.9 kcal/mol), it is obvious that $PH_3$ dissociation takes place after B−B activation.

As seen in Figure 6, in general, the potential energy profile of the $C_2H_4$ diboration reaction is rather similar to the PES of the $C_2H_2$ reaction. After the oxidative addition of B−B to $Pt(PH_3)_2$ and dissociation of a $PH_3$, alkene can coordinate to the three-coordinate complex **XIo** to give **XIIo**. The coordination energy is calculated to be 14.9 kcal/mol somewhat larger than $C_2H_2$ (12.9 kcal/mol). Then the insertion of ethylene into Pt−B bond takes place with 22.9 kcal/mol barrier **XIVo**, while the insertion barrier is calculated to be only 9.0 kcal/mol for acetylene. The process, **XIIa/o** → **XIVa/o**, is calculated to be *endothermic* by 4.1 kcal/mol for ethylene while it is highly, 28.1 kcal/mol, *exothermic* for acetylene. Similar to the $C_2H_2$ case, the isomerization of B−C−C in **XIVo** and recoordination of $PH_3$ group to form **XVIo** which is next step of the reaction 2 is calculated to be 23.9 kcal/mol exothermic. The corresponding value for the reaction 1 is 21.3 kcal/mol. The elimination process is also similar; the elimination barriers are calculated to be 12.2 and 14.0 kcal/mol, for reactions 2 and 1, respectively. The total exothermicity of the entire reaction is smaller for ethylene, 41.7 kcal/mol vs 60.8 kcal/mol for acetylene.

*Thus, it is clear that the different catalytic behavior of $Pt(PH_3)_2$ for two substrates, $C_2H_2$ and $C_2H_4$, is the result of the differences in relative stability of the complexes **XIIa/o** and **XIVa/o** and the barrier heights corresponding to the insertion of hydrocarbons into the Pt−B bond at **XIIIa/o**.* In order to understand the sources of these differences, we recall once again the processes taking place during the **XIIa/o** → **XIVa/o** rearrangement: cleavage of the C−C $\pi$-bond and the Pt−B bond, as well as formation of the B−C and the Pt−C $\sigma$-bonds. We artificially separate these processes into the following three steps, as shown in Scheme 2:.

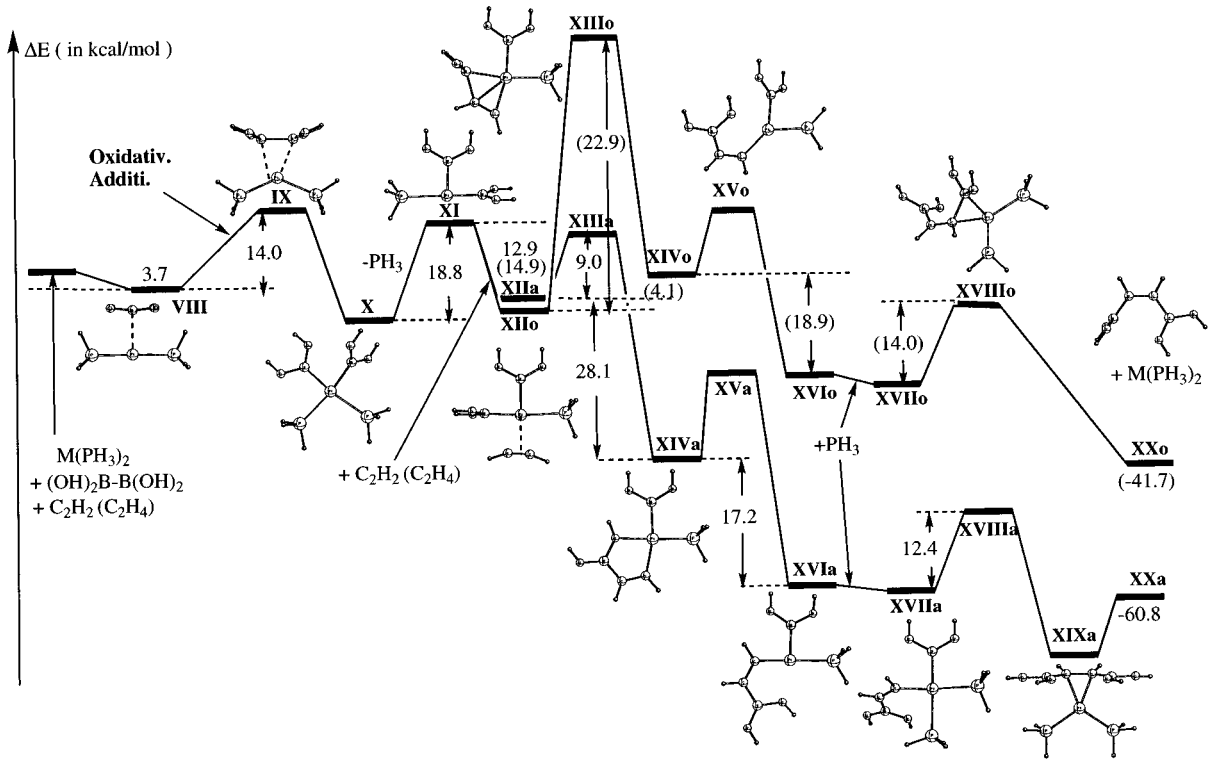


**Figure 6.** Potential energy profiles for path A of the entire catalytic cycle of reactions 1 and 2 (in parentheses).

**Scheme 2**

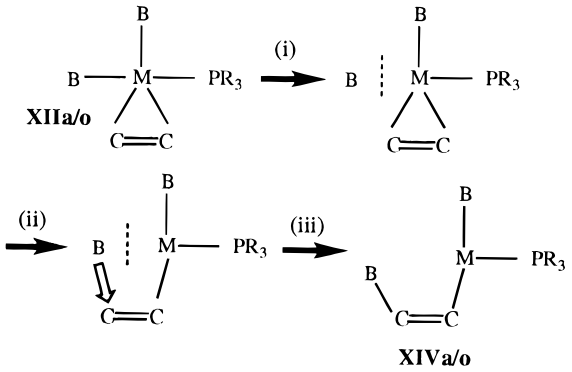


(i) The energy loss in the process of breaking the Pt−B bond, which is modeled by dissociating the reacting $B(OH)_2$ fragment from **XIIa/o** and keeping other parameters unchanged except that the *trans*-Pt−P distance is shortened to that in **XIVa/o**; (ii) the energy loss in the rearrangement of the Pt−$C_2H_x$ fragment, which is estimated by changing the geometry of $C_2H_x$ in the structure of (i) to that in **XIVa/o** while keeping other parameters unchanged; (iii) the binding energy of $B(OH)_2$ to $C_2H_x$·Pt, which is estimated as the energy difference from the structure of (ii) to **XIVa/o**. Obviously these are very crude and artificial estimates but should provide some hints about the origin of the difference between $C_2H_2$ and $C_2H_4$ systems. These single point calculations are done at the B3LYP/I level. For step i, the "binding energy" of $B(OH)_2$ to Pt is calculated to be 98 kcal/mol for **XIIa** and 99 kcal/mol for **XIIo**; the Pt−B bonds are similar between the two systems. This is also obvious from the similar Pt−B and Pt−P bond lengths in **XIIa** and **XIIo**. For step ii, the energy needed for the deformation of the geometries of Pt−$C_2H_x$ fragment is estimated to be 21 and 38 kcal/mol for $C_2H_2$ and $C_2H_4$, respectively. In other words, the dissociation of the $\pi$-bond of acetylene takes place much more easily than the $\pi$-bond of alkene. For step iii, the energy of $\sigma$ bond formation between $B(OH)_2$ and $C_2H_x$ is calculated to be 147 and 138 kcal/mol for acetylene ($x = 2$) and ethylene ($x = 4$), respectively. It should be emphasized again that these numbers should not be taken quantitatively because the other geometrical parameters are fixed and the "intermediates" in those artificial steps are certainly far from being optimized. However, we can clearly see a qualitative picture. The difference between the relative stabilities of **XIIa/o** and **XIVa/o** mainly comes from two origins. As the first origin, in step ii the change of geometry in $C_2H_4$ is less favorable than in $C_2H_2$ by 16 kcal/mol. In this step, the interaction between $C_2H_x$ and Pt changes from a $\pi$ fashion to a $\sigma$ fashion, a set of $\pi$ bonds is completely broken, and the hybridization of the second carbon is changed artificially by fixing the geometry to that in **XIVa/o**. As the second origin, in step (iii) the B−C $\sigma$ bond is weaker with $C_2H_4$ by 9 kcal/mol compared with $C_2H_2$. We assign this difference to the fact that the remaining $\pi$ orbital in $C_2H_2$ can enhance the C−B bond by donating electron density into the empty $\pi$ orbital of the $B(OH)_2$ group. The difference in the exothermicity of the total reaction between $C_2H_2$ and $C_2H_4$ system can also be understood with a similar argument.

## VII. Conclusions

We may draw the following conclusions from the current study.

(1) The B3LYP/II//B3LYP/I approach provides quite reliable agreement with available experiment and CCSD(T)//B3LYP/I method for the energy gap between low-lying $^1S(s^0d^{10})$ and $^3D(s^1d^9)$ states of the Pt atom and the binding energies for Pt−$BH_2$, Pt−$PH_3$, Pt−$B(OH)_2$, and $PH_3$−Pt($PH_3$) bonds.

(2) Path A of the Pt(0)-catalyzed alkyne and alkene diboration reactions, (1) and (2), is found to be more favorable than path B and proceeds via the following steps: (a) coordination of $(OH)_2B-B(OH)_2$ to $Pt(PH_3)_2$, (b) oxidative addition of the B−B bond to Pt, (c) dissociation of one of the phosphine ligands, (d) coordination of alkyne/alkene to form $\pi$-complexes, (e) migratory insertion of alkyne/alkene into a Pt−B bond, (f) migration of $CHCHB(OH)_2$ (or $CH_2CH_2B(OH)_2$) group to become *cis* to $B(OH)_2$, (g) recoordination of the second phosphine ligand to Pt *cis* to the first $PH_3$, and (h) elimination of *cis*-$CHCH[B(OH)_2]_2$ (or $CH_2CH_2[B(OH)_2]_2$). The rate-determining step is found to be phosphine dissociation step c.

(3) The main differences between alkyne and alkene diboration reactions on Pt(0) lie in the relative stabilities of the complexes $(PH_3)(BR_2)_2Pt(C_2H_X)$, **XIIa/o**, and $(PH_3)(BR_2)Pt(C_2H_XBR_2)$, **XIVa/o** (where $x = 2$ and 4), and in the barrier **XIIIa/o** corresponding to the insertion of the alkyne/alkene fragments into the Pt−B bond. For alkyne diboration reaction 1, **XIVa** is 28.1 kcal/mol *lower* than **XIIa** with a *modest insertion barrier* of 9.0 kcal/mol, while for alkene diboration reaction 2, **XIVo** is 4.1 kcal/mol *higher* than **XIIo** with a *large barrier* of 22.9 kcal/mol. These differences have been explained in terms of a smaller substrate deformation energy and a larger B−C $\sigma$ bond energy for alkyne than for alkene in **XIIIa/o**.

(4) The coordination of acetylene and ethylene to $Pt(PH_3)_2$ is calculated to be more favorable than the oxidative addition of $(OH)_2B-B(OH)_2$ to $Pt(PH_3)_2$. However, for highly substituted alkyne/alkene and diborane derivatives, the oxidative addition of the B−B bond to $Pt(PH_3)_2$ becomes more favorable than the coordination of alkyne/alkene to $Pt(PH_3)_2$

**Acknowledgment.** The authors express their gratitude to Prof. T. B. Marder for providing the manuscript of a paper and very useful and intensive discussions of these and related results. The use of computational facilities and programs at the Emerson Center is acknowledged. The present research is in part supported by grants (CHE-9409020 and CHE96-27775) from the National Science Foundation. The Phillips Petroleum Co. Graduate Fellowship to Q.C. is acknowledged.

OM960860H